DOI 10.1111/j.1365-2133.2008.08540.x

Extremely low frequency electromagnetic field enhances human keratinocyte cell growth and decreases proinflammatory chemokine production

G. Vianale, M. Reale, P. Amerio, M. Stefanachi,* S. Di Luzio*† and R. Muraro

*Department of Oncology and Neurosciences and *Department of Clinical Science and Bioimaging, University 'G. d'Annunzio' of Chieti-Pescara, 66013 Chieti, Italy*

†ITAB – University Foundation 'G. d'Annunzio', Chieti University, Chieti, Italy

Correspondence
Raffaella Muraro.
E-mail: muraro@unich.it

Accepted for publication
5 January 2008

Key words
chemokines, electromagnetic field, keratinocytes, NF-κB, real-time polymerase chain reaction

Conflicts of interest
None declared.

Summary

Background Proliferation and differentiation of keratinocytes are central processes in tissue regeneration after injury. Chemokines, produced by a wide range of cell types including keratinocytes, play a regulatory role in inflammatory skin diseases. Several studies have shown that an electromagnetic field (EMF) can influence both inflammatory processes and repair mechanisms including wound healing on different tissue models.

Objectives To elucidate the effect of extremely low frequency EMF (ELF-EMF) on keratinocyte proliferation and production of chemokines [RANTES, monocyte chemoattractant protein (MCP)-1, macrophage inflammatory protein (MIP)-1α and interleukin (IL)-8] in order to evaluate a potential therapeutic use of magnetic fields.

Methods The human keratinocyte cell line HaCaT was exposed at 1 mT, 50 Hz for different lengths of time and compared with unexposed control cells. Cell growth and viability were evaluated at different exposure times by cell count and trypan blue exclusion. Chemokine production and expression were analysed by enzyme-linked immunosorbent assay (ELISA) and by real-time polymerase chain reaction. Total NF-κB p65 was quantified by ELISA.

Results Significantly increased growth rates were observed after 48 h of EMF exposure as compared with control cells, while no difference in cell viabilities were detected. Gene expression and release of RANTES, MCP-1, MIP-1α and IL-8 were significantly reduced after 72 h of exposure. NF-κB levels became almost undetectable after only 1 h of EMF exposure, and were inversely correlated with cell density.

Conclusions Our results show that ELF-EMF modulates chemokine production and keratinocyte growth through inhibition of the NF-κB signalling pathway and thus may inhibit inflammatory processes. ELF-EMF could represent an additional therapeutic approach in the treatment of skin injury.

The effects on human health of exposure to an extremely low frequency electromagnetic field (ELF-EMF) have been widely debated, the main concerns focusing on their carcinogenic potential and relationship with immune system functions. However, controlled EMF exposures are still widely used for the treatment of some pathological conditions to stimulate neural regeneration, tissue and bone repair.[1,2] In fact, EMFs have been shown to enhance circulation by increasing blood flow,[3] favour bone formation and healing through the increase of osteoblast maturation[4] and enhance the recovery of tensile strength after tendon injury.[5]

The biological effects of EMFs are dependent on frequency, amplitude, timing and length of exposure, but are also related to intrinsic susceptibility/responsiveness of different cell types.[6] In bone marrow-derived macrophages, EMFs induce a significant increase in phagocytic activity, small differences in O_2^- production, but no differences in nitric oxide (NO) production. No effects on cytokine production in mononuclear

blood cells after EMF exposure have been detected,[7] while a growth inhibitory effect has been shown in T lymphocytes.[8] A previous study demonstrated downregulation of inducible NO synthase and upregulation of monocyte chemoattractant protein (MCP)-1 in human peripheral blood monocytes exposed to 1 mT, 50 Hz EMF.[9] Chow and Tung[10] have demonstrated that magnetic fields can actually enhance the efficiency of DNA repair.

In general, repair stimulation is one of the stronger and better documented biological effects of EMFs. The variability of the therapeutic results and therefore of exposure windows of the different tissues for repair relate to the involvement of several cell types that may differentially respond to the EMF stimulus. For example, repair by EMF has been morphologically documented in skin and soft tissue.[11] Other reports highlighted the effect on vascularization, reduction in wound depth by granulation tissue, and reduced inflammatory cell migration and infiltration.[12] However, contradictory results have been observed in human clinical studies involving the use of EMFs to treat chronic ulcers.[13] Chronic ulcers are a significant cause of morbidity and mortality in the elderly population, as healing is frequently difficult to achieve. One of the underlying mechanisms responsible for the failure of chronic wound healing is an out-of-control inflammatory response that is self-sustaining.[14]

Indeed, tissue healing is a complex process involving epidermal, dermal as well as inflammatory cell proliferation and migration, mediated and modulated by paracrine and/or autocrine production of chemokines.[15] The processes of keratinocyte proliferation and differentiation represent the central and final event in tissue regeneration leading to the formation of a massive bulk of cells, necessary to cover the wounded area.[16]

Chemokines are low molecular weight chemotactic cytokines that have been shown to play a relevant role in inflammatory events, such as transendothelial migration and accumulation of leucocytes at the site of damage. In addition, they modulate a number of biological responses, including enzyme secretion, cellular adhesion, cytotoxicity and T-cell activation and tissue regeneration.[17,18] Chemokines are divided into four families, based on the arrangement of cysteine residues, two of which have been extensively studied: the CXC family, including interleukin (IL)-8, and the CC family, including MCP-1, macrophage inflammatory protein (MIP)-1 and RANTES (Regulated upon Activation, Normal T cell Expressed and Secreted). Chemokines are produced by a variety of cells including monocytes, T lymphocytes, neutrophils, fibroblasts, endothelial cells and epithelial cells. Keratinocytes have been shown to produce RANTES, MCP-1, MIP-1 and IL-8.[19]

In the present study, we investigated the influence of EMF exposure on cell growth and production of the chemokines IL-8, MCP-1, MIP-1α and RANTES, as well as the transcription factor NF-κB, in the human keratinocyte cell line HaCaT. Our results suggest that the constitutive IL-8, MCP-1, MIP-1α and RANTES production by HaCaT cells is significantly downregulated by EMF exposure. These data, paralleled by the early reduction of NF-κB levels, support the hypothesis that EMF exposure could favour wound healing by increasing keratinocyte growth rate and reducing the production of proinflammatory molecules.

Materials and methods

Electromagnetic field exposure system

All experiments were performed using a sinusoidal 50-Hz EMF at a flux density of 1 mT (r.m.s.) produced by an electromagnetic generator (Hewlett-Packard (Palo Alto, CA, U.S.A.) model 33120 with stability higher than 1% both in frequency and in amplitude), as previously reported.[10] A current flow of 1·20 A (I_{eff}) passed through a 160-turn solenoid coil of length l = 0·22 m and radius a = 0·06 m. The copper wire thickness was $1{\cdot}25 \times 10^{-3}$ m. The generator was connected to a power amplifier (Denon POA 2800, NAD Electronics Ltd, London, U.K.). Cells were placed in the central part of the solenoid, which presented the highest degree of field homogeneity (98%). Magnetic field strength and distribution within the solenoid were measured with a Hall-effect probe connected to a Gaussmeter (MG-3D; Walker Scientific Inc., Worcester, MA, U.S.A.). Geomagnetic field intensity inside the incubator was about 40 μT; in the same area, the environmental magnetic noise due to power line (50 Hz) was about 7 μT (r.m.s.). The experimental setup for exposure to magnetic field is shown in Figure 1.

The immortalized human keratinocytes HaCaT were grown in complete medium (Dulbecco's modified Eagle's medium supplemented with 10% heat-inactivated fetal bovine serum, 100 U mL^{-1} penicillin and 100 μg mL^{-1} streptomycin). Cells, derived from the same freeze-down batch, were thawed, grown in a flask, seeded at densities of 10×10^3 and 50×10^3 cells per well on to six-well tissue culture plates and cultured in two different incubators, in the same room, at

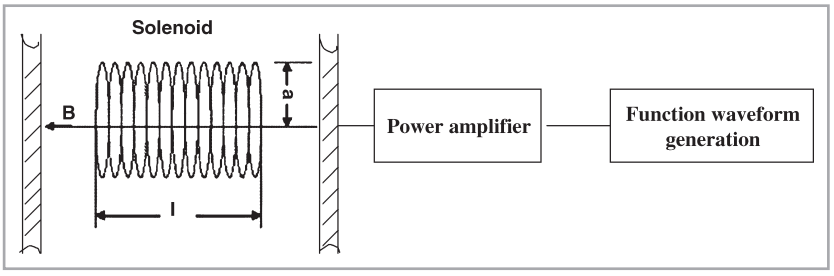

Fig 1. Schematic representation of the exposure system. The solenoid was placed inside the cell incubator. The diameter of the solenoid was a = 0·06 m, and its length was l = 0·22 m. The number of solenoid turns was 160, and the diameter of the copper wire was $1{\cdot}25 \times 10^{-3}$ m. B indicates the direction of the magnetic field.

37 °C in a humidified atmosphere of 5% CO_2. Both control and exposed culture experiments were run simultaneously and under exactly the same conditions. HaCaT cells were exposed to a 50-Hz EMF at a flux density of 1 mT (r.m.s.) produced by an electromagnetic generator and located on a grid to allow air circulation in the central part of the solenoid where the highest EMF homogeneity (98%) was present. Control nonexposed cell plates were placed in a different incubator where only the environmental magnetic field could be detected.

Taking into account that the solenoid inside the incubator may generate power and thus increase the internal temperature, the thermal effect of EMF exposure on the incubator and on the culture medium was monitored for the entire length of the EMF exposure both in preliminary experiments and every hour for the first 24 h, and then randomly until the end of the study (72 h). The temperature inside the incubator was monitored by a built-in thermometer (temperature, $t = 37 \pm 0{\cdot}2$ °C), while the temperature of the cell medium was measured using a specially designed thermoresistor (HD 9216; Delta OHM, Padua, Italy). The low-level Joule heating was efficiently dissipated by the fan system inside the incubator as Δt was $\leq 0{\cdot}1308$ °C in the medium of exposed cells.

Cell viability was not influenced by field exposure. More than 98% of cells were viable, as determined by trypan blue dye exclusion at the beginning of the culture, and more than 90% were viable before cells were collected.

Cell growth curves

Cells were seeded at densities of 10×10^3 and 50×10^3 cells per well in separate six-well plates for control and EMF-exposed cultures and placed into different incubators as described. HaCaT cells were exposed at 1 mT, 50 Hz in the solenoid region, where the field gradient was 3%. The cultures were kept under continuous EMF exposure for the entire length of the experiments (1, 4, 12, 24, 48, 72, 96 h) without medium replacement. Control cells were grown simultaneously in a different cell incubator for the same time and under identical conditions except for EMF. At the selected intervals, cells were counted and viability determined by trypan blue dye exclusion.

EMF exposures and control experiments were repeated at least five times in triplicate to ensure and verify the reproducibility of the results. All experiments were run in parallel for EMF-exposed and control cells.

Chemokines assay

MCP-1, MIP-1α and RANTES release levels were evaluated by commercial SearchLight Multiplex Assays sandwich enzyme-linked immunosorbent assay (ELISA) kits (Endogen, Woburn, MA, U.S.A.) following the manufacturer's instructions in conditioned medium after 1, 4, 12 and 72 h of culture. Before assay, aliquots of tissue culture supernatant were thawed and diluted (1 : 10) with the sample diluents, in order to obtain values lower than the upper limit of the calibration range. The plates were imaged using a specialized cooled CCD instrument. The integrated density values of spots for known standards were used to generate standard curves. Density values for unknown samples were assessed using the standard curve for each analyte to calculate actual values in pg mL^{-1}. The detection limit of the assay was $< 0{\cdot}8$ pg mL^{-1} for MCP-1, $< 3{\cdot}1$ pg mL^{-1} for MIP-1α and $< 0{\cdot}4$ pg mL^{-1} for RANTES. The intra- and interassay reproducibility was > 90%. Experiments with duplicate values differing by > 10% were repeated. IL-8 release was evaluated by commercial ELISA kits (Endogen) following the manufacturer's instructions; the detection limit of the assay was < 2 pg mL^{-1}.

NF-κB assay

Cells were washed twice with cold phosphate-buffered saline, centrifuged at 4 °C and resuspended in 10 mmol L^{-1} Tris pH 7·4, 100 mmol L^{-1} NaCl, 1 mmol L^{-1} ethylenediamine tetraacetic acid, 1 mmol L^{-1} EGTA, 1 mmol L^{-1} NaF, 1% Triton X-100, 0·1% sodium dodecyl sulphate, 10% glycerol, 2 mmol L^{-1} Na_3VO_4, 20 mmol L^{-1} $Na_4P_2O_7$, 1 mmol L^{-1} phenylmethylsulphonyl fluoride, 1 mg mL^{-1} leupeptin and aprotinin, and vortexed at 10-min intervals and kept on ice for 30 min. Cell lysates were centrifuged for 10 min at 10 000 *g* at 4 °C and 200 μg mL^{-1} of total protein used to quantify total NF-κB p65 using the BioSource ELISA kit (Camarillo, CA, U.S.A.). The detection limit of the assay was < 50 pg mL^{-1}.

RNA extraction and reverse transcription–polymerase chain reaction analysis

Total RNA was extracted from HaCaT cell cultures using the TRIzol reagent (Invitrogen, Life Technologies, Paisley, U.K.) according to the manufacturer's protocol. The RNA concentration was estimated by measuring the absorbance at 260 nm using a Bio-Photometer (Eppendorf AG, Hamburg, Germany), and RNA samples were kept frozen at –80 °C until use. Purified RNA was electrophoresed on a 1% agarose gel to assess the integrity of the purified RNA. Three micrograms of RNA was reverse transcribed into cDNA using a High Fidelity Superscript reverse transcriptase commercially available kit (Applied Biosystems, Foster City, CA, U.S.A.), according to the manufacturer's instructions. Programmes and primers for the measurement of steady state levels of mRNA of the other gene products were as follows: glyceraldehyde-3-phosphate dehydrogenase (GAPDH) forward: 5′-ATG CAT CTC AGA GGT GCA GG-3′; GAPDH reverse: 5′-ACT GCT GGT GGA AGA TGT CG-3′ (cDNA length is 275 bp); RANTES forward: 5′-CAG AGG ATC AAG ACA GCA CG-3′; RANTES reverse: 5′-CAA GCT AGG ACA AGA GCA AGC-3′ (cDNA length is 394 bp); MIP-1α forward: 5′-TTC TCT GCA TCA CTT GCT GC-3′; MIP-1α reverse: 5′-TCC ATA GAA GAG GTA GCT GTG G-3′ (cDNA length is 329 bp); MCP-1 forward: 5′-AAT GAA GCT CGC ACT CTC G-3′; MCP-1 reverse: 5′-GAG TGA GTG TTC AAG

TCT TCG G-3′ (cDNA length is 338 bp). All polymerase chain reactions (PCRs) were performed in PCR-express cyclers (Hybaid, Heidelberg, Germany). The PCR amplification programme was as follows: an initial period of 5 min at 95 °C, followed by a variable number of cycles of 30 s denaturation at 95 °C, 30 s annealing at 60 °C and finally 30 s of extension at 72 °C. The programme was terminated with a period of 10 min at 72 °C. To be within the exponential phase of the semiquantitative PCR reaction,[20] the appropriate number of cycles was newly established for every set of samples. PCR products were separated by gel electrophoresis on 1·5% agarose gels and visualized by ethidium bromide staining. All gels were scanned and the normalized intensities of all reverse transcription (RT)-PCR products were determined by the BioRad gel documentation system (BioRad, Hercules, CA, U.S.A.). Mean ± SEM intensities were calculated for all RT-PCR experiments.

Real-time polymerase chain reaction system

Total RNA was extracted in the same way as for RT-PCR. Quantitative real-time PCR assay was carried out in an Eppendorf Mastercycler EP Realplex (Eppendorf AG). Preliminary PCR reactions were run to optimize the concentration and ratio of each primer set. For all the cDNA templates 2 μL was used in a 20-μL real-time PCR amplification system of SYBR Green Real Master Mix Kit according to the manufacturer's directions. Primers for human RANTES, MIP-1α and MCP-1 genes and GAPDH as control were designed using GeneWorks software (IntelliGenetix, Inc., Mountain View, CA, U.S.A.). Similar amplification procedures and data computation were followed as described above. No PCR products were generated from genomic vs. cDNA template.

The fluorescence intensity of the double-strand-specific SYBR Green, reflecting the amount of formed PCR product, was monitored at the end of each elongation step. Melting curve analysis was performed to confirm the purity of the PCR products. Relative expression of RANTES, MIP-1α and MCP-1 was normalized to GAPDH using the ΔCT method [relative expression = $2^{-\Delta CT}$, where $\Delta CT = C_{T(\text{RANTES, MIP-1}_\alpha \text{ MCP-1})} - C_{T(\text{GAPDH})}$].[20,21] Predicted cycle threshold values were exported directly into Excel worksheets for analysis. Relative changes in gene expression were determined by the $2^{-\Delta\Delta CT}$ method as described previously[22] and reported as the difference (n-fold) relative to the value for a calibrator cDNA (control) prepared in parallel with the experimental cDNAs. Data are representative of three different experiments each run in triplicate and are presented as the mean ± SEM of triplicates. DNA was denatured at 95 °C for 2 min followed by 40 cycles of 30 s at 95 °C together with 30 s at 60 °C. The experiments were repeated twice with consistent results.

Statistical analysis

Differences in growth curves were compared by the two-way Kruskal–Wallis test. Exposed vs. control chemokine levels at each time point were compared by the nonparametric Mann–Whitney U-test with Bonferroni correction. NF-κB levels were correlated with cell growth by Spearman test.

Results

Keratinocyte growth curves

In order to evaluate the effect of EMF on keratinocyte growth, HaCaT cells were seeded and exposed to 50 Hz, 1 mT EMF in the solenoid region for different times (Fig. 1). In parallel, HaCaT cells were grown under identical conditions, but in a different incubator to ensure the absence of EMF interference and were used in all experiments as control.

Figure 2 shows the growth curves obtained by counting cells at 4, 12, 24, 48, 72 and 96 h. EMF-exposed keratinocytes demonstrated an increased growth rate compared with control cells ($P < 0{\cdot}001$). However, only a slight increase was observed in the first 24 h, while cell growth was significantly increased following prolonged exposure (at 48 and 72 h: $P = 0{\cdot}005$ and $P = 0{\cdot}001$, respectively). No differences in cell viability were noted between exposed and control cells, as reported in Figure 2.

Effect of electromagnetic field exposure on chemokine release and mRNA expression

Cell culture supernatants collected at the time of cell counts were used to analyse chemokine production levels. Table 1 illustrates chemokine levels detected after 4, 12 and 72 h of EMF exposure. Significant differences were observed after 72 h of exposure. The production of RANTES and IL-8 displayed the most significant reductions in exposed cells,

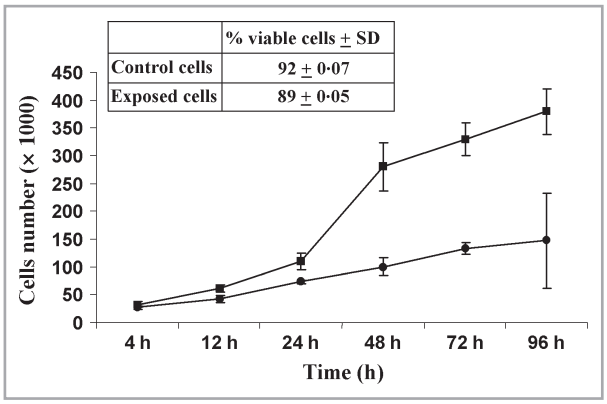

Fig 2. Growth curves of human HaCaT keratinocytes exposed to extremely low frequency electromagnetic field (squares) and controls (circles). Curves represent the mean ± SD of five different experiments run in triplicate. Differences in growth curves were compared by two-way Kruskal–Wallis test ($P < 0{\cdot}001$); individual time points were compared by nonparametric Mann–Whitney U-test with Bonferroni correction ($P = 0{\cdot}005$ at 48 h and $P = 0{\cdot}001$ at 72 h, respectively).

Table 1 RANTES, monocyte chemoattractant protein (MCP)-1, macrophage inflammatory protein (MIP)-1α and interleukin (IL)-8 levels (mean ± SD) in 1 mT, 50 Hz electromagnetic field (EMF) exposed and control HaCaT cells

	1 h	4 h	12 h	72 h	P-value
RANTES (pg mL^{-1})					
EMF	ND	3·3 ± 0·71	1·6 ± 0·15	88·2 ± 1·4	< 0·001
Control	ND	5·5 ± 0·02	5·1 ± 1·05	441 ± 12·9	
MCP-1 (pg mL^{-1})					
EMF	ND	1·7 ± 0·05	3 ± 1·30	65·6 ± 3·8	0·002
Control	ND	3·3 ± 0·20	6·2 ± 0·10	214 ± 5·15	
MIP-1α (pg mL^{-1})					
EMF	ND	ND	ND	54·6 ± 1·35	0·008
Control	ND	ND	ND	166·4 ± 10·4	
IL-8 (pg mL^{-1})					
EMF	ND	1·0 ± 0·03	1·5 ± 0·03	285 ± 4	0·008
Control	ND	64·8 ± 1·05	259·9 ± 3	1481 ± 2	

ND, not detectable. Statistical analyses were performed by nonparametric Mann–Whitney U-test comparing levels at 72 h in exposed vs. unexposed cultures.

exhibiting a fivefold decrease ($P < 0·001$ and $P = 0·008$, respectively), while MCP-1 and MIP-1α displayed threefold reductions ($P = 0·002$ and $P = 0·008$, respectively). Note that the levels measured in the conditioned media represent the total amounts produced over the test period (72 h), as no medium replacement was performed.

To determine whether the decreased chemokine levels in the exposed cells were dependent on alterations at the gene transcription level, RT-PCR experiments were performed using specific primers. Figure 3 illustrates a representative RT-PCR experiment (Fig. 3a) and the mean intensity of the densitometric gel analyses of all RT-PCR experiments (Fig. 3b). Based on RT-PCR relative levels, quantitative real-time PCR experiments were performed for RANTES and MCP-1. In control cells the expression levels of RANTES and MCP-1 increased from 4 to 72 h of growth, thus confirming the increased release into the medium. EMF-exposed keratinocytes showed a similar decrease of expression both at 4 h and at 72 h of exposure, as compared with control

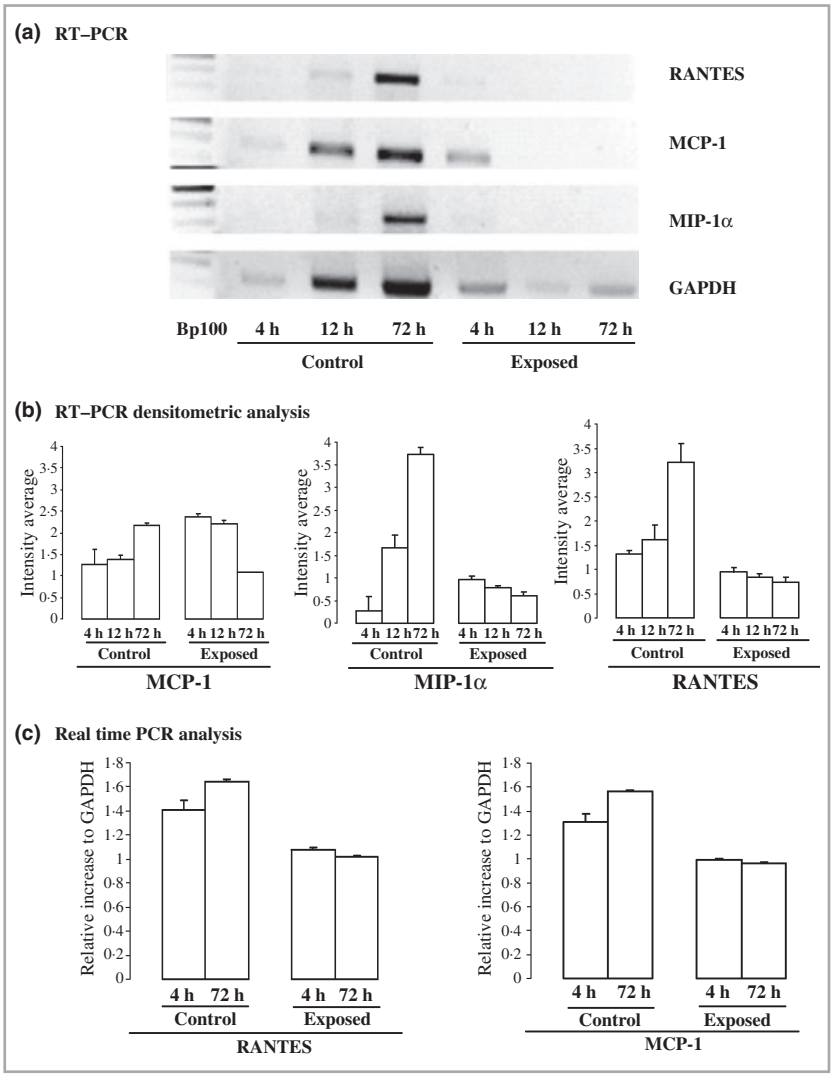

Fig 3. Effect of exposure to extremely low frequency electromagnetic field (EMF) on chemokine expression in HaCaT cells. RANTES, monocyte chemoattractant protein (MCP)-1 and macrophage inflammatory protein (MIP)-1α mRNA expression were determined by reverse transcription–polymerase chain reaction (RT-PCR) and real-time PCR. (a) Total RNA was subjected to RT-PCR. Lane 1, HaCaT (4 h – unexposed control cells); lane 2, HaCaT (12 h – unexposed control cells); lane 3, HaCaT (72 h – unexposed control cells); lane 4, HaCaT (4 h – EMF exposed); lane 5, HaCaT (12 h – EMF exposed); lane 6, HaCaT (72 h – EMF exposed). GAPDH, glyceraldehyde-3-phosphate dehydrogenase. (b) Densitometric analysis of semiquantitative RT-PCR products determined using a BioRad gel documentation system (mean ± SEM). (c) Relative increase of RANTES and MCP-1 mRNA expression (mean ± SEM) by real-time PCR at 4 h and 72 h of exposure. Time points were compared by nonparametric Mann–Whitney U-test with Bonferroni correction ($P = 0·008$).

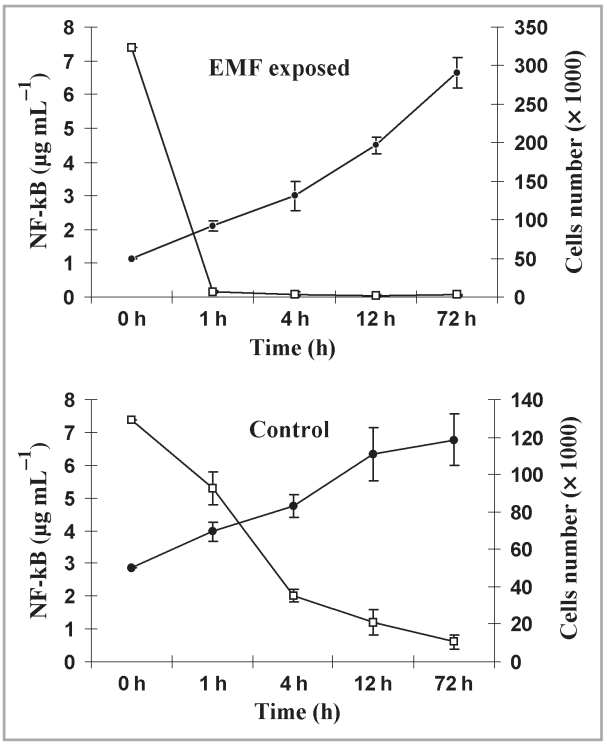

Fig 4. Effect of electromagnetic field exposure on activated NF-κB levels in HaCaT cells. Open circles, NF-κB levels; closed circles, HaCaT cell numbers. Results are shown as mean ± SD. NF-κB levels were correlated with cell growth by Spearman test (control cells: $\rho = -1$; exposed cells: $\rho = -0{\cdot}9$). Exposed vs. control levels at each time point were compared by nonparametric Mann–Whitney U-test with Bonferroni correction ($P = 0{\cdot}005$, $P = 0{\cdot}006$, $P = 0{\cdot}056$, $P = 0{\cdot}064$ at 1, 4, 12 and 72 h, respectively).

cells (percentage reduction for RANTES at 4 h: 23·6%; 72 h: 38%; and for MCP-1 at 4 h: 24%; 72 h: 39%) (Fig. 3c).

Effect of electromagnetic field exposure on NF-κB activation

In order to ascertain a potential effect of EMF on the transcription factor NF-κB, we analysed the activated NF-κB p65 levels in total cell extract from proliferating exposed and control HaCaT keratinocytes. Figure 4 compares NF-κB p65 levels in proliferating keratinocytes exposed to EMF and in proliferating control cells. Control keratinocytes show a progressive reduction of activated NF-κB levels inversely correlated with cell number ($\rho = -1$, $P < 0{\cdot}001$). In contrast, NF-κB levels in EMF-exposed HaCaT cells dramatically decreased ($P = 0{\cdot}037$) after only 1 h of exposure. Thus, NF-κB levels in EMF-exposed cells are not correlated with cell growth/number. In fact, while in unexposed keratinocytes NF-κB levels decreased over a time period of 72 h, in exposed keratinocytes NF-κB levels became almost undetectable after only 1 h of EMF exposure (at 1 h $P = 0{\cdot}005$).

Discussion

Magnetic field exposure enhances wound healing by reducing inflammatory cell infiltration and by enhancing the substitution of granulation tissue with dense connective tissue.[12] In addition, several lines of evidence indicate that extremely low ELF-EMF modulates growth and keratinocyte differentiation and interferes with cellular adhesion, thus favouring wound healing.[23] In experimental models, advanced stages of wound repair are associated with a shift towards macrophage and anti-inflammatory chemokine profiles in parallel with a decrease of proinflammatory chemokines such as RANTES, MCP-1, MIP-1α and IL-8.[24] As skin is usually exposed to electromagnetic radiation more than other tissues, HaCaT cells, a spontaneously immortalized human keratinocyte cell line, was chosen as an *in vitro* model to investigate the effect of ELF-EMF on keratinocyte growth and on production and expression of proinflammatory molecules.

In this study we showed that ELF-EMF exposure increased the proliferative activity of HaCaT cells, reduced their production of chemokines and reduced transcription factor NF-κB p65 levels.

In control keratinocytes, chemokine expression and production were related to cell number: higher chemokine levels were detected in high density HaCaT cultures. In contrast, chemokine levels in keratinocytes exposed to ELF-EMF were not directly linked to cell growth, as they were significantly lower, as compared with the control cells, even with a threefold increased cell number.

The effects of ELF-EMF exposure on keratinocyte growth are consistent with those reported for other cell lines.[23,25] Nevertheless, the susceptibility to the proliferative effects of ELF-EMF varies widely among cell types, as no single or common mechanisms have been implicated for all tissues. Keratinocyte proliferation is modulated by at least two pathways: one NF-κB dependent and one NF-κB independent (e.g. Ca^{2+}). Some authors reported that NF-κB exerts an inhibitory influence on keratinocyte growth.[26] Several studies have suggested that EMF exposure can alter intracellular Ca^{2+} homeostasis. Significant increases in intracellular Ca^{2+} levels have been observed in various immune-cell models,[27] but conflicting observations have emerged from studies of neuroendocrine cells.[28]

Unexposed HaCaT cells showed a progressive reduction of NF-κB levels during the time course experiment, reaching very low levels at 72 h. In contrast, the exposure to ELF-EMF had an almost immediate effect on NF-κB levels, which became nearly undetectable after only 1 h. In addition, exposed cells displayed a more rapid growth rate than control cells. Thus, an inverse relationship between NF-κB levels and cell growth in exposed and unexposed cells is suggested.

A selective inhibition of the NF-κB signalling pathway by ELF-EMF may be involved in the decrease of chemokine production. An inverse relationship between NF-κB levels and

chemokine production in both nonexposed and exposed HaCaT cells was immediately apparent.

Our results suggest that ELF-EMF exposure, interfering with many cellular processes, may be included in the plethora of stimuli that modulate NF-κB activation (including proinflammatory cytokines such as tumour necrosis factor-α and IL-1β, chemokines, phorbol 12-myristate 13-acetate, growth factors, lipopolysaccharide, ultraviolet irradiation, viral infection, as well as various chemical and physical stresses).

In vitro studies have demonstrated diverse cellular responses to EMF that may be relevant to wound healing. For example, migration of cultured fibroblasts and epithelial cells in perpendicular alignment to applied electrical fields is a well-established phenomenon.[29] During re-epithelialization, keratinocytes proliferate to form a dense hyperproliferative epithelium to cover the wound, and repair requires resolution of the inflammatory response. However, whereas the knowledge about mechanisms and molecules inducing and perpetuating the inflammatory responses is constantly increasing, mechanisms that downregulate these activities are still poorly understood.

As it is well accepted that an excessive or prolonged inflammatory response results in poor and late healing, any approach that could downregulate proinflammatory chemokines may have potentially relevant therapeutic application. Our findings highlight the role of ELF-EMF in downregulation of chemokine production paralleled by decreased levels of activated NF-κB.

It is widely accepted that *in vitro* keratinocyte model systems at low and high density can be compared with early and late phases of the re-epithelialization process. As ELF-EMF modulates keratinocyte proliferation and expression of inflammatory chemokines, it could be suggested that ELF-EMF could be used to treat inflammatory skin conditions. ELF-EMF exposure, a noninvasive therapy, could represent an additional therapeutic approach in the treatment of skin injury and to increase the performance of bioengineered skin substitutes as a new strategy for repair. Furthermore, our model could help to optimize the EMF field amplitude, timing and length of exposure in order to achieve clinical results.

Acknowledgments

This study was supported in part by grants from the Ministero dell'Università e della Ricerca (MIUR).

References

1 Kheifets L, Shimkhada R. Childhood leukemia and EMF: review of the epidemiologic evidence. *Bioelectromagnetics* 2005; **7**:S51–9.
2 Bassett CA. Beneficial effects of electromagnetic fields. *J Cell Biochem* 1993; **51**:387–93.
3 Gmitrov J, Ohkubo C, Okano H. Effect of 0.25 T static magnetic field on microcirculation in rabbits. *Bioelectromagnetics* 2002; **23**: 224–9.
4 Linovitz RJ, Pathria M, Bernhardt M *et al.* Combined magnetic fields accelerate and increase spine fusion: a double-blind randomized, placebo controlled study. *Spine* 2002; **27**:1383–9.
5 Strauch B, Patel MK, Rosen DJ *et al.* Pulsed magnetic field therapy increases tensile strength in a rat Achilles' tendon repair model. *J Hand Surg [Am]* 2006; **3**:1131–5.
6 Tenuzzo B, Chionna A, Panzarini E *et al.* Biological effects of 6 mT magnetic fields: a comparative study in different cell types. *Bioelectromagnetics* 2006; **27**:560–70.
7 Ikeda K, Shinmura Y, Mizoe H *et al.* No effects of extremely low frequency magnetic fields found on cytotoxic activities and cytokine production of human peripheral blood mononuclear cells *in vitro*. *Bioelectromagnetics* 2003; **24**:21–31.
8 Norimura T, Imada H, Kunugita N *et al.* Effects of strong magnetic fields on cell growth and radiation response of human T-lymphocytes in culture. *J UOEH* 1993; **15**:103–12.
9 Reale M, De Lutiis MA, Patruno A *et al.* Modulation of MCP-1 and iNOS by 50-Hz sinusoidal electromagnetic field. *Nitric Oxide* 2006; **15**:50–7.
10 Chow K, Tung WL. Magnetic field exposure enhances DNA repair through the induction of DnaK/J synthesis. *FEBS Lett* 2000; **478**:133–6.
11 Ottani V, DePasquale P, Franchi M *et al.* Effects of pulsed extremely-low-frequency magnetic fields on skin wounds in the rat. *Bioelectromagnetics* 1988; **9**:53–62.
12 Bertolino G, de Freitas A, de Oliveira BK *et al.* Macroscopic and histological effects of magnetic field exposition in the process of tissue reparation in Wistar rats. *Arch Dermatol Res* 2006; **298**:121–6.
13 Ravaghi H, Flemming K, Cullum N, Olyaee Manesh A. Electromagnetic therapy for treating venous leg ulcers. *Cochrane Database Syst Rev* 2006; **2**:CD002933.
14 Menke NB, Ward KR, Witten TM *et al.* Impaired wound healing. *Clin Dermatol* 2007; **25**:19–25.
15 Santoro MM, Gaudino G. Cellular and molecular facets of keratinocyte reepithelization during wound healing. *Exp Cell Res* 2005; **304**:274–86.
16 Sivamani RK, Garcia MS, Isseroff RR. Wound re-epithelialization: modulating keratinocyte migration in wound healing. *Front Biosci* 2007; **12**:2849–68.
17 Zlotnick A, Yoshie O. Chemokines: a new classification and their role in immunity. *Immunity* 2000; **12**:121–7.
18 Murdoch C, Finn A. Chemokine receptors and their role in inflammation and infectious diseases. *Blood* 2000; **10**:3032–43.
19 Iocono JA, Colleran KR, Remick DG *et al.* Interleukin-8 levels and activity in delayed-healing human thermal wounds. *Wound Repair Regen* 2000; **8**:216–25.
20 Wang AM, Doyle MV, Mark DF. Quantification of mRNA by the polymerase chain reaction. *Proc Natl Acad Sci U S A* 1989; **86**:9717–21.
21 Wang J, Xi L, Hunt JL *et al.* Expression pattern of chemokine receptor 6 (CCR6) and CCR7 in squamous cell carcinoma of the head and neck identifies a novel metastatic phenotype. *Cancer Res* 2004; **64**:1861–6.
22 Livak KJ, Schmittgen TD. Analysis of relative gene expression data using real-time quantitative PCR and the $2^{-\Delta\Delta CT}$ method. *Methods* 2001; **25**:402–8.
23 Manni V, Lisi A, Pozzi D *et al.* Effects of extremely low frequency (50 Hz) magnetic field on morphological and biochemical properties of human keratinocytes. *Bioelectromagnetics* 2002; **23**:298–305.
24 Fivenson DP, Faria DT, Nickoloff BJ *et al.* Chemokine and inflammatory cytokine changes during chronic wound healing. *Wound Repair Regen* 1997; **5**:310–32.

25 Wei M, Guizzetti M, Yost M *et al.* Exposure to 60-Hz magnetic fields and proliferation of human astrocytoma cells *in vitro*. *Toxicol Appl Pharmacol* 2000; **162**:166–76.
26 Lindström E, Lindström P, Berglund A *et al.* Intracellular calcium oscillations induced in a T-cell line by a weak 50 Hz magnetic field. *J Cell Physiol* 1993; **156**:395–8.
27 Barbier E, Dufy B, Veyret B. Stimulation of Ca^{2+} influx in rat pituitary cells under exposure to a 50 Hz magnetic field. *Bioelectromagnetics* 1996; **17**:303–11.
28 Takao T, Yudate A, Das S *et al.* Expression of NF-κB in epidermis and the relationship between NF-κB activation and inhibition of keratinocyte growth. *Br J Dermatol* 2003; **148**:680–8.
29 Stiller MI, Pak GH, Shupack JL *et al.* A portable pulsed electromagnetic field (PEMF) device to enhance healing of recalcitrant venous ulcers: a double-blind, placebo-controlled clinical trial. *Br J Dermatol* 1992; **127**:147–54.

